© 2014. Published by The Company of Biologists Ltd | Development (2014) 141, 1757-1766 doi:10.1242/dev.104422

RESEARCH ARTICLE

Endothelial cell-derived non-canonical Wnt ligands control vascular pruning in angiogenesis

Claudia Korn[1,*], Beate Scholz[1,2,*], Junhao Hu[1], Kshitij Srivastava[1,2], Jessica Wojtarowicz[1,2], Tabea Arnsperger[1,3], Ralf H. Adams[4,5], Michael Boutros[3,6,‡], Hellmut G. Augustin[1,2,7,‡,§] and Iris Augustin[3,6,‡]

ABSTRACT

Multiple cell types involved in the regulation of angiogenesis express Wnt ligands. Although β-catenin dependent and independent Wnt signaling pathways have been shown to control angiogenesis, the contribution of individual cell types to activate these downstream pathways in endothelial cells (ECs) during blood vessel formation is still elusive. To investigate the role of ECs in contributing Wnt ligands for regulation of blood vessel formation, we conditionally deleted the Wnt secretion factor *Evi* in mouse ECs (Evi-ECKO). Evi-ECKO mice showed decreased microvessel density during physiological and pathological angiogenesis in the postnatal retina and in tumors, respectively. The reduced microvessel density resulted from increased vessel regression accompanied by decreased EC survival and proliferation. Concomitantly, survival-related genes were downregulated and cell cycle arrest- and apoptosis-inducing genes were upregulated. *EVI* silencing in cultured HUVECs showed similar target gene regulation, supporting a mechanism of EC-derived Wnt ligands in controlling EC function. ECs preferentially expressed non-canonical Wnt ligands and canonical target gene expression was unaffected in Evi-ECKO mice. Furthermore, the reduced vascularization of Matrigel plugs in Evi-ECKO mice could be rescued by introduction of non-canonical Wnt5a. Treatment of mouse pups with the non-canonical Wnt inhibitor TNP470 resulted in increased vessel regression accompanied by decreased EC proliferation, thus mimicking the proliferation-dependent Evi-ECKO remodeling phenotype. Taken together, this study identified EC-derived non-canonical Wnt ligands as regulators of EC survival, proliferation and subsequent vascular pruning during developmental and pathological angiogenesis.

KEY WORDS: Angiogenesis, Evi, Vessel regression, Wnt, Mouse

INTRODUCTION

Formation of blood vessels includes the processes of sprouting angiogenesis, vessel maturation and remodeling. During angiogenic sprouting, tip cell migration is followed by stalk cell proliferation and lumen formation. Subsequently, maturing vascular networks are stabilized by basement membrane deposition and pericyte recruitment. To match vessel perfusion with the metabolic demand of the tissue, the primitive vascular plexus undergoes remodeling to form a hierarchically structured vasculature. Whereas VEGF/VEGFR, Delta/Notch and Angiopoietin/Tie signaling are well established regulators of vascular sprouting and network formation, Wnt ligands have only more recently been studied as vascular morphogens (Potente et al., 2011).

The Wnt family consists of 19 highly conserved glycoproteins, which signal via Frizzled receptors to initiate different intracellular downstream cascades controlling cell fate, proliferation, apoptosis, migration and polarity. Wnt signaling pathways can be classified into canonical (β-catenin dependent) and non-canonical (β-catenin-independent) branches, including planar cell polarity (PCP) and Wnt/Ca^{2+} signaling (Clevers and Nusse, 2012).

So far, primarily downstream effects after Wnt ligand binding have been investigated in the vasculature by endothelial β-catenin manipulation, global Frizzled-4 or Nrarp deletion (Cattelino et al., 2003; Phng et al., 2009; Corada et al., 2010; Descamps et al., 2012). Canonical Wnt signaling plays an established role during early steps of embryonic stem cell to EC differentiation (Wang et al., 2006), remodeling of the embryonic vessels (Cattelino et al., 2003; Corada et al., 2010) and establishment of organ-specific vasculatures (Liebner et al., 2008; Stenman et al., 2008; Daneman et al., 2009). Furthermore, canonical Wnt signaling has been described to interfere with vessel regression by stimulating EC proliferation during postnatal retinal angiogenesis (Phng et al., 2009) and to promote pericyte recruitment, thereby inducing tumor vessel normalization (Reis et al., 2012). By contrast, evidence for non-canonical Wnt signaling during angiogenesis is only beginning to emerge (Masckauchan et al., 2006; Cirone et al., 2008; Descamps et al., 2012). On the one hand, non-canonical Wnt ligands have been shown to suppress angiogenesis during retinal vascularization and wound healing (Stefater et al., 2011, 2013). On the other hand, Wnt5a has been described as a pro-angiogenic factor promoting EC proliferation, migration, survival and network formation (Masckauchan et al., 2006; Cirone et al., 2008; Descamps et al., 2012). However, the upstream cellular regulators controlling canonical and non-canonical Wnt downstream signaling in ECs have not been identified. As Wnt ligands are expressed by a variety of cells involved in the regulation of angiogenesis, including ECs, pericytes, macrophages and neural cells, it is of major importance to resolve the Wnt contribution of these cell types to gain a better understanding of the complex Wnt signaling network during blood vessel formation (Goodwin et al., 2006; Stenman et al., 2008; Stefater et al., 2011). So far, only macrophages have been reported to provide canonical as well as non-canonical Wnt ligands to control vessel formation. Whereas macrophage-derived non-canonical Wnt ligands regulate angiogenesis in an indirect manner, the source for Wnt ligands that directly induce downstream signaling in ECs

[1]Division of Vascular Oncology and Metastasis, German Cancer Research Center (DKFZ-ZMBH Alliance), Heidelberg 69221, Germany. [2]Department of Vascular Biology and Tumor Angiogenesis (CBTM), Medical Faculty Mannheim, Heidelberg University, Mannheim 68167, Germany. [3]Division of Signaling and Functional Genomics, German Cancer Research Center (DKFZ), Heidelberg 69221, Germany. [4]Department of Tissue Morphogenesis, Max Planck Institute for Molecular Biomedicine, Muenster 48149, Germany. [5]Faculty of Medicine, University of Muenster, Muenster 48149, Germany. [6]Department of Cell and Molecular Biology (CBTM), Medical Faculty Mannheim, Heidelberg University, Mannheim 68167, Germany. [7]German Cancer Consortium, Heidelberg 69221, Germany.
*These authors contributed equally to this work
‡These authors contributed equally to this work

[§]Author for correspondence (augustin@angiogenese.de)

Received 1 October 2013; Accepted 21 February 2014

Development (2014) 141, 1757-1766 doi:10.1242/dev.104422

continues to be elusive (Rao et al., 2007; Stefater et al., 2011, 2013). In particular, the role of ECs in contributing Wnt ligands to regulate angiogenesis has not been discriminated from the impact of any bystander cell types.

An essential component of the Wnt secretion machinery is the highly conserved seven-pass transmembrane protein Evenness Interrupted (Evi; also known as Wntless, Wls), which acts as a cargo receptor required for pan-Wnt protein exocytosis from the Golgi to the cell surface (Bartscherer et al., 2006). In the absence of Evi, Wnt ligand secretion is inhibited in the Wnt-producing cell. Based on the unique role of Evi as a gatekeeper of Wnt secretion, the present study was aimed at postnatally deleting *Evi* in ECs in mouse in order to clarify in a definite genetic setting the role of endothelial-derived autocrine-acting Wnt ligands in regulating vessel formation and remodeling.

RESULTS

Evi-ECKO mice show reduced vascularization in postnatal retinal and tumor angiogenesis

In order to study the role of the vascular endothelium as a source of Wnt ligands in controlling vessel formation and remodeling, *Evi floxed/floxed* mice were crossed with *Cdh5CreERT2* mice (Evi-ECKO). The morphology of the retinal vasculature at postnatal day (P) 6 was visualized by staining with isolectin B4 (IB-4) after tamoxifen-mediated postnatal *Evi* deletion in ECs. Retinal vascularization was decreased, as indicated by reduced vessel area and radial expansion from the optic nerve to the periphery, in Evi-ECKO compared with wild-type littermate mice (Evi-WT) (Fig. 1A,E,I). A detailed analysis of the vessel structure in Evi-ECKO mice revealed a reduction in the density of the vascular network correlating with a decreased number of junctions and branches (Fig. 1B,F,J). To analyze whether the reduced vessel area was accompanied by a decreased number of ECs, the total EC number was determined by counting cells positive for the EC-specific transcription factor ERG1 (Ets-related gene 1). The uniform ERG1 expression in ECs in different retinal regions, including the sprouting front, central retina, artery and vein (supplementary material Fig. S1A-D), classified ERG1 as valid tool for counting of ECs. The ERG1 staining revealed a significantly reduced number of ECs per retina area (Fig. 1C,G) in Evi-ECKO compared with littermate WT mice. However, normalizing the number of $ERG1^+$ ECs to the vessel area showed no difference between WT and Evi-ECKO mice, demonstrating a linear correlation between the $ERG1^+$ EC number and the vessel area and an equal numerical distribution of ECs between Evi-ECKO and WT mice (supplementary material Fig. S1E).

To study the consequences of *Evi* deletion in ECs on pathological angiogenesis, Lewis lung carcinoma (LLC) cells were subcutaneously (s.c.) injected in Evi-ECKO and control mice and the growing tumor vasculature was visualized by staining for CD31 (Pecam1). Tumor vessel area and tumor vessel density were significantly reduced in Evi-ECKO mice compared with littermate WT controls (Fig. 1D,K,H). Concomitantly, the number of small vessels (<500 μm^2 CD31 area) was reduced, whereas the number of larger vessels (>500 μm^2 CD31 area) was not affected (Fig. 1L), indicating that primarily immature microvessels are unstable in the absence of EC-derived Wnt ligands. Taken together, EC-derived Wnt ligands controlled physiological as well as pathological angiogenesis.

EC-derived Evi regulates vessel remodeling by controlling EC proliferation and apoptosis

To investigate further if vessel formation or remodeling was affected by loss of endothelial *Evi*, sprouting angiogenesis was analyzed in Evi-ECKO mice. The number of tip cells per mm vessel front was reduced in Evi-ECKO mice (supplementary material Fig. S2A,C). However, high resolution analysis of tip cells did not identify differences in the number of filopodia per tip cell in Evi-ECKO mice, suggesting that tip cell function and, thus, the process of vessel sprouting per se was not disturbed in Evi-ECKO mice (supplementary material Fig. S2A,E). Furthermore, co-staining of desmin and IB-4 revealed no difference in pericyte coverage between Evi-ECKO and littermate WT mice (supplementary material Fig. S2B,D). Along the same line, fluorescence-activated cell sorting (FACS) of Evi-ECKO and WT lung ECs showed similar *Pdgfb* expression, indicating that pericyte recruitment and, thus, vessel maturation were not affected by loss of endothelial *Evi* (supplementary material Fig. S2F).

Because the processes of vessel sprouting and maturation were not significantly altered in Evi-ECKO mice and the loss of small vessels in the tumor vasculature of Evi-ECKO mice suggested an increase in vessel regression, the impact of EC-specific *Evi* deletion on vessel remodeling was investigated in the postnatal retina. During vessel remodeling, redundant branches are selected for regression and subsequent constriction. After luminal occlusion, ECs retract and leave empty basement membrane sleeves behind (Baffert et al., 2006). Co-staining of IB-4 and the basement membrane component collagen IV (ColIV) revealed an increased number of empty basement membrane sleeves ($IB4^-ColIV^+$) in Evi-ECKO mice, indicating that vessel regression was increased upon deletion of endothelial *Evi* (Fig. 2A,E). As vessel regression has been correlated with a shift of vasoactive gene expression towards a vasoconstrictory phenotype (Lobov et al., 2011), we analyzed vasoconstrictor gene expression in FACS-sorted lung ECs. Both angiotensinogen (*Agt*) and endothelin receptor A (*Ednra*) were found to be upregulated in Evi-ECKO mice, further confirming the increase in vessel remodeling upon *Evi* deletion in ECs (Fig. 2I). Because the total EC number was reduced and vessel remodeling was increased in Evi-ECKO mice, we analyzed apoptosis of ECs as a possible cause for increased vessel regression. Staining of IB-4 together with TUNEL (terminal deoxynucleotidyl transferase dUTP nick end labeling) or with cleaved caspase-3 staining identified an increase in EC apoptosis in Evi-ECKO compared with littermate WT controls (Fig. 2B,C,F,G). To link the morphological changes in the Evi-ECKO retinal vasculature to downstream signaling events, gene expression was analyzed in FACS-sorted P6 lung ECs. The classical pro-apoptotic gene *Bax* and the apoptosis-related gene *Stat2* were found to be upregulated (Fig. 2J). Expression of *Tek*, which controls EC survival (Augustin et al., 2009), was also downregulated in Evi-ECKO vessels, suggesting a role of Wnt ligands in controlling EC survival (Fig. 2K).

The reduced EC number in Evi-ECKO mice may not only be due to decreased EC survival but could have also resulted from impaired EC proliferation leading to increased vessel remodeling. Hence, EC proliferation was analyzed in Evi-ECKO mice by co-staining of IB-4 and bromodeoxyuridine (BrdU). These experiments revealed a reduction of EC proliferation in Evi-ECKO retinal vessels (Fig. 2D,H). Similarly, impaired EC proliferation correlated with increased gene expression of the cyclin-dependent kinase inhibitor *Cdkn1a* in FACS-sorted lung ECs (Fig. 2L). In conclusion, EC-derived Wnt ligands did not affect vessel sprouting and maturation, but controlled EC survival and proliferation and, thus, vessel stabilization.

Non-canonical Wnt signaling regulates vessel stabilization

To analyze whether EC-derived Wnt-dependent vessel stabilization was mediated by canonical and/or non-canonical Wnt signaling, Wnt

Development (2014) 141, 1757-1766 doi:10.1242/dev.104422

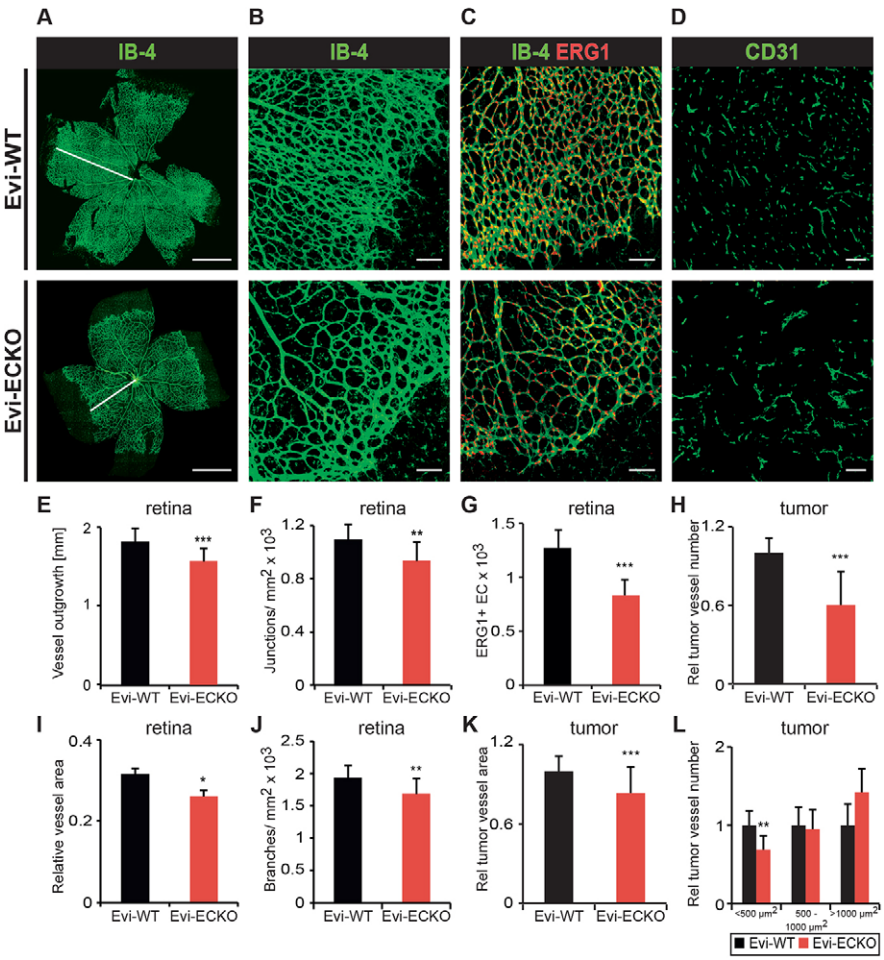

Fig. 1. Reduced retinal vascularization and EC number in Evi-ECKO mice. (A,B) Representative images of the total retinal vasculature (A) and the sprouting front (B) stained with IB-4 in Evi-WT and Evi-ECKO retinas. (C) Representative images of the retinal vasculature co-stained with IB-4 and ERG1 in Evi-WT and Evi-ECKO mice. (D) Representative images of the vasculature stained for CD31 in Evi-WT and Evi-ECKO LLC tumor sections. (E-L) Quantifications of retina vessel outgrowth (E; n=16), junctions/mm^2 vessel area (F; n=16), ERG1$^+$ ECs per retina area (G; n=8), relative tumor vessel number (H; n=15), relative retinal vessel area (I; n=16), branches/mm^2 vessel area (J; n=16), relative tumor vessel area (K; n=15) and relative number of small, medium and big tumor vessels (L; n=15). Scale bars: 1 mm (A); 100 µm (B-D). Data are shown as mean±s.d. (E-H,J,K) or mean±s.e.m. (I,L). *P<0.05, **P<0.01, ***P<0.001.

ligand expression was analyzed in FACS-sorted lung and retinal ECs (Fig. 3A; supplementary material Fig. S3A). Retinal as well as lung ECs showed a prominent non-canonical Wnt ligand signature (Fig. 3B,C). Whereas retinal ECs expressed the non-canonical ligands *Wnt5a* and *Wnt5b* as well as the canonical *Wnt2*, lung ECs expressed the non-canonical Wnts *Wnt5a*, *5b* and *11* and weakly expressed *Wnt2*. These non-canonical Wnt ligands were furthermore upregulated in lung and retinal EC of P6 pups compared with adult mice, arguing for a role of β-catenin-independent Wnt signaling in regulating active angiogenesis (Fig. 3B,C). To test further for a role of the canonical Wnt pathway in EC-autonomous control of vessel stabilization, the expression of typical canonical target genes, including *Axin*2, *Ccnd1*, *Myc* and *Vegfa*, was analyzed in Evi-ECKO mice (Fig. 3D). No difference in canonical target gene expression was detected. Notch target gene expression was reported to be upregulated upon activation of canonical Wnt signaling in ECs (Corada et al., 2010). However, screening different target genes of the Notch pathway did not show any downregulation of Notch target genes in Evi-ECKO mice, supporting a β-catenin-independent regression phenotype (Fig. 3E).

To validate further the non-canonical phenotype, Matrigel plugs containing basic fibroblast growth factor (bFGF) and Wnt5a or bFGF only were implanted into Evi-ECKO and control littermates. Analysis of the plug vasculature revealed a reduction of the vessel area and number in bFGF-containing plugs in Evi-ECKO mice in comparison with plugs in WT mice (Fig. 3F-H). The reduced vascularization of plugs in Evi-ECKO mice could be rescued by addition of Wnt5a to the plugs, confirming that the absence of non-canonical Wnt signaling was responsible for the vascular defects in Evi-ECKO mice. Thus, ECs expressed non-canonical Wnt ligands to induce β-catenin-independent downstream Wnt signaling required for vessel stabilization.

Pharmacological inhibition of non-canonical Wnt signaling in WT mice phenocopies the Evi-ECKO phenotype

To validate further the non-canonical phenotype of Evi-ECKO mice, WT mice were treated with the angiogenesis inhibitor TNP470, which blocks non-canonical Wnt signaling by inhibiting methionine aminopeptidase 2 (MetAP2). It thereby induces a PCP-defective phenotype characterized by disturbed EC proliferation, polarity and network formation *in vitro* and *in vivo*. TNP470-triggered PCP inhibition has been confirmed by showing that TNP470 treatment was phenocopied by PCP-defective and rescued by non-canonical constitutively active Dvl2 (disheveled 2) mutant constructs (Ingber et al., 1990; Zhang et al., 2006; Cirone et al., 2008). In the present study, postnatal treatment of mice with TNP470 resulted in decreased vascularization of the mouse retina as indicated by a reduced relative vessel area and impaired radial expansion (Fig. 4A,E,I). As in Evi-ECKO mice, TNP470 treatment resulted in decreased vascular network complexity showing a reduced number of junctions and branches per vessel area (Fig. 4B,F,J). The non-canonical character of the TNP470-induced vascularization defect correlated with unchanged expression of canonical target genes, including *Axin2*, *Myc* and *Ccnd1* as well as multiple Notch target genes (supplementary material Fig. S4A,B).

Inhibition of non-canonical Wnt signaling by TNP470 treatment reduced the total number of ECs (Fig. 4D,H) and increased vessel

Development (2014) 141, 1757-1766 doi:10.1242/dev.104422

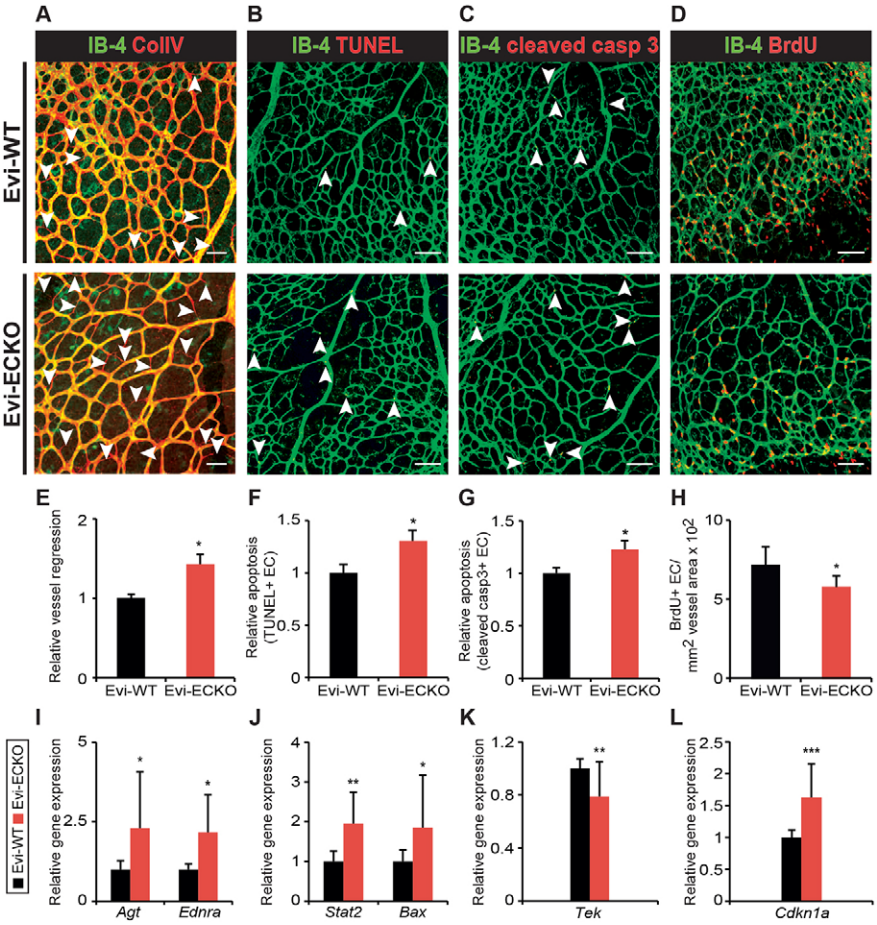

Fig. 2. Increased vessel regression in Evi-ECKO mice as a consequence of reduced survival and proliferation. (A-D) Representative images of the vasculature co-stained with IB-4 and CollV (A), IB-4 and TUNEL (B), IB-4 and cleaved caspase-3 (C), and IB-4 and BrdU (D) in Evi-WT and Evi-ECKO retinas. CollV^{+} empty sleeves, TUNEL^{+} ECs and cleaved caspase-3^{+} ECs are indicated by arrowheads. (E-H) Quantifications of relative vessel regression (E; n=11), relative number of TUNEL^{+}IB-4^{+} cells per retina area (F; n=31), relative number of cleaved caspase-3^{+}IB-4^{+} cells per retina area (G; n=18) and total number of BrdU^{+}IB-4^{+} cells per retina area (H; n=18). (I-L) Gene expression analyses of FACS-sorted lung ECs from Evi-WT and Evi-ECKO mice (I-L). Scale bars: 50 µm (A); 100 µm (B-D). Data are shown as mean±s.d. (H-L) or mean±s.e.m. (E-G). *P<0.05, **P<0.01, ***P<0.001.

regression (Fig. 5A,E), similar to Evi-ECKO mice, which again correlated with decreased EC proliferation and upregulation of *Cdkn1a* gene expression in FACS-sorted mouse lung ECs (Fig. 5D,H; supplementary material Fig. S4C). However, postnatal TNP470 treatment did not reveal differences in apoptosis as assessed by TUNEL and by cleaved caspase-3 staining (Fig. 5B,C,F,G). Similarly, *Stat2*, *Bax* and *Tek* gene expression were not altered in lung ECs of TNP470-treated mice (supplementary material Fig. S4C).

In addition to vessel remodeling, vessel sprouting and maturation were analyzed in TNP470-treated mice. Upon TNP470 treatment, the number of tip cells per mm vessel front was reduced, which, in contrast to Evi-ECKO mice, was accompanied by a deceased number of filopodia per tip cell (Fig. 4C,G,K). However, similar to Evi-ECKO mice, no defects in pericyte coverage as well as *Pdgfb* gene expression were observed upon TNP470 treatment (Fig. 4L; supplementary material Fig. S5A,B). In conclusion, TNP470 treatment of WT mice phenocopied the remodeling phenotype of Evi-ECKO mice as a consequence of reduced EC proliferation but not of increased apoptosis.

Regulation of EC survival and proliferation-associated gene expression is driven by autocrine-acting Wnt ligands

The analysis of postnatal retinal angiogenesis in Evi-ECKO and littermate WT mice suggested an autocrine role of non-canonical Wnt ligands in controlling vessel remodeling. To confirm further the autocrine regulation of Wnt-dependent EC survival signaling and to exclude adverse effects of bystander cells such as pericytes, macrophages, neural cells or astrocytes *in vivo*, the role of non-canonical Wnt ligands was further explored in cultured HUVECs. Screening of WNT gene expression in HUVECs revealed expression of canonical *WNT2B* and *WNT3*, non-canonical *WNT5A* as well as the dual pathways inducing *WNT4* (Fig. 6A). However, silencing of *EVI* in HUVECs (Fig. 6B) did not show downregulation of the canonical target gene *AXIN2* (Fig. 6E), supporting an autocrine regulation of non-canonical Wnt signaling in maintaining EC function. Similar to the gene regulation in Evi-ECKO mice, Evi siRNA treatment of HUVECs resulted in upregulation of the pro-apoptotic genes *STAT2* and *BAX* as well as the downregulation of *TEK* (Fig. 6C,D,F). Furthermore, *EVI* silencing in HUVECs also increased expression of the cell cycle arrest-inducing factor *CDKN1A* (Fig. 6G). In conclusion, deletion of Evi in ECs *in vitro* as well as *in vivo* resulted in similar regulation of target gene expression, promoting an autocrine control of EC survival and proliferation and, thus, vessel remodeling.

DISCUSSION

Canonical Wnt signaling has been described to promote vessel stabilization. Evidence for non-canonical Wnt signaling in controlling vascular development is only recently emerging. However, the identity of the Wnt-providing cells in the vascular system and in particular the role of the ECs in cell-autonomously regulating Wnt signaling is still unclear. Employing a definite genetic approach, we show in the present study that: (1) EC-derived Wnt ligands control endothelial network formation in the retina model and in LLC tumors; (2) EC-derived Wnt ligands inhibit vessel regression; (3) EC proliferation and apoptosis as well as *Cdkn1a*, *Bax*, *Stat2* and *Tek* gene expression are regulated by EC-derived Wnt ligands; (4) EC-specific deletion of *Evi* does not affect the processes of vessel sprouting and maturation; (5) retinal ECs express a primarily

Development (2014) 141, 1757-1766 doi:10.1242/dev.104422

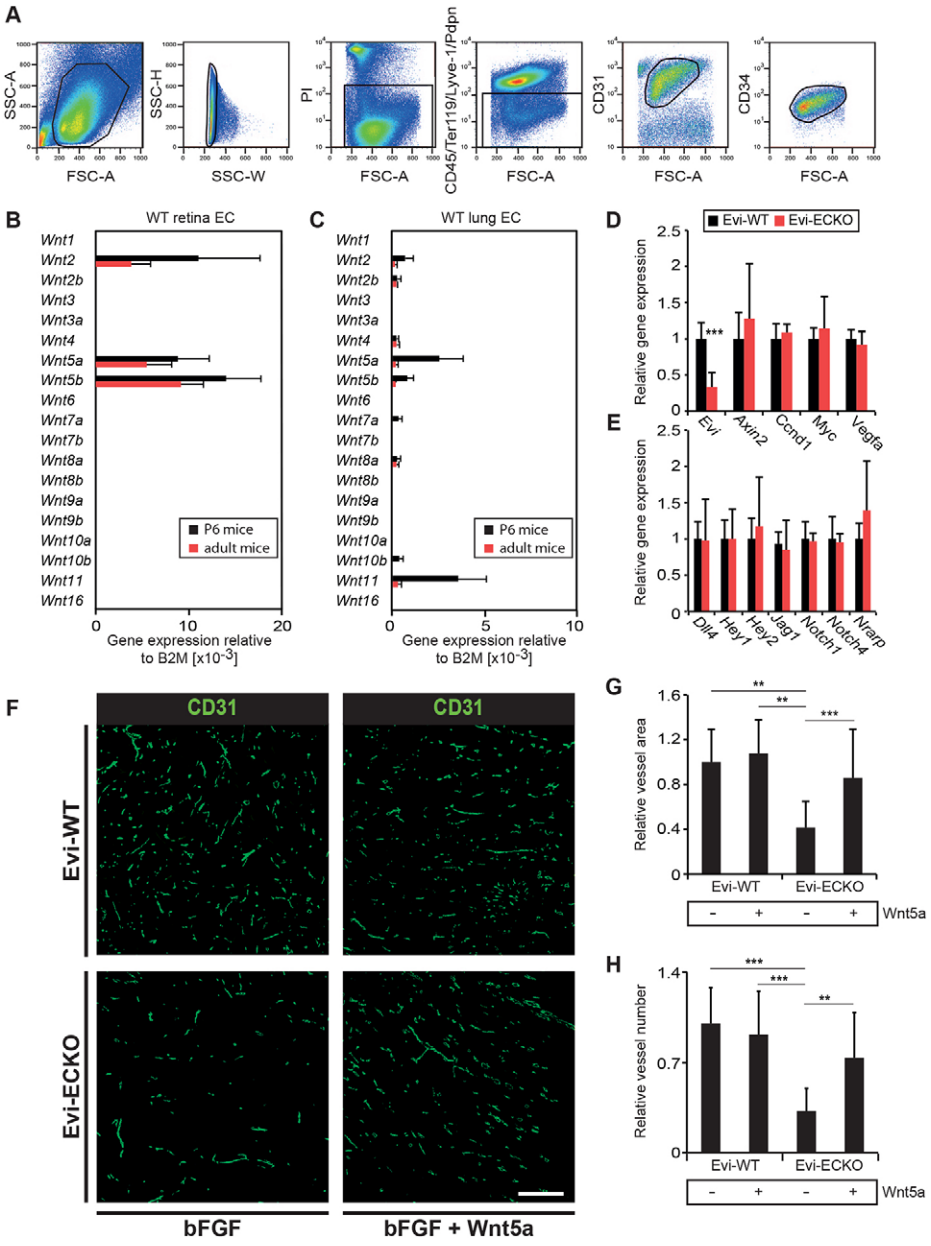

Fig. 3. EC-derived Wnt ligands regulate non-canonical Wnt downstream signaling in ECs. (A) Representative FACS sorting scheme for the isolation of viable (PI^-) lung ECs. $CD45^-Ter119^-Lyve1^-Pdpn^-CD31^+CD34^+$ cells were sorted for gene expression analysis. (B,C) Wnt gene expression pattern of ECs isolated from retina (B) or lung (C) of WT P6 and adult mice. (D,E) Gene expression analyses of canonical target genes (D) and Notch genes (E) in lung ECs of Evi-WT and Evi-ECKO mice. (F) Representative images of the vasculature of Matrigel plugs containing bFGF or bFGF and Wnt5a in Evi-WT and Evi-ECKO mice stained with CD31. (G,H) Quantifications of the relative vessel area (G; n=8) and relative vessel number (H; n=8) in the Matrigel plugs. Scale bar: 200 µm. Data are shown as mean±s.d. (B-E,G,H). $^{**}P$<0.01, $^{***}P$<0.001.

non-canonical Wnt signature, which induces β-catenin-independent downstream signaling; and (6) inhibition of non-canonical Wnt signaling by TNP470 treatment of mice mimics the increased regression and decreased proliferation phenotype of Evi-ECKO mice and also interferes with EC sprouting (Fig. 7).

We have in this study identified a key role of EC-derived Wnt ligands as regulators of vessel regression by promoting EC survival. Previous studies have linked vessel regression to increased apoptosis. For instance, depletion of vascular endothelial growth factor (VEGF) after primary network formation induced vessel regression correlating with detachment and increased apoptosis of ECs (Alon et al., 1995; Baffert et al., 2006). Furthermore, leukocytes promote pruning of retinal vessels by inducing EC apoptosis and FGD5/Cdkn1a/p53 signaling interferes with EC survival, stimulating subsequent vessel regression (Ishida et al., 2003; Cheng et al., 2012). However, whether vessel regression is initially triggered by apoptosis due to withdrawal of survival factors or whether regression is followed by apoptosis of retracted ECs that have lost cell-cell and cell-matrix contact remains elusive. The present study identified reduced numbers of ECs in Evi-ECKO mice in P6 retinal vessels, supporting the hypothesis that loss of Evi-mediated Wnt secretion from ECs results in reduced survival signaling, thus selecting ECs for apoptosis. EC death is then followed by vessel rearrangement to adopt the vascular network to the reduced cell number. The impaired survival upon *Evi* deletion in ECs was accompanied by downregulation of *Tek*, which is known to mediate angiopoetin-1 (Angpt1)-induced Akt/phosphatidylinositol 3-kinase-dependent survival signaling (Augustin et al., 2009), as well as upregulation of *Bax* and *Stat2*, which are involved in pro-apoptotic signal transduction (Kim and Lee, 2007; Martinou and Youle, 2011).

This study describes for the first time the regulation of vessel remodeling by non-canonical Wnt ligands as primarily non-canonical Wnt ligands were found to be expressed in retina and lung ECs and canonical target genes were largely unchanged upon endothelial *Evi* deletion. Yet, signaling via Norrin (Ndp) and Fzd4, which promotes retinal angiogenesis by inducing Wnt ligand-independent canonical Wnt signaling, could compensate a possible canonical branch of the

Development (2014) 141, 1757-1766 doi:10.1242/dev.104422

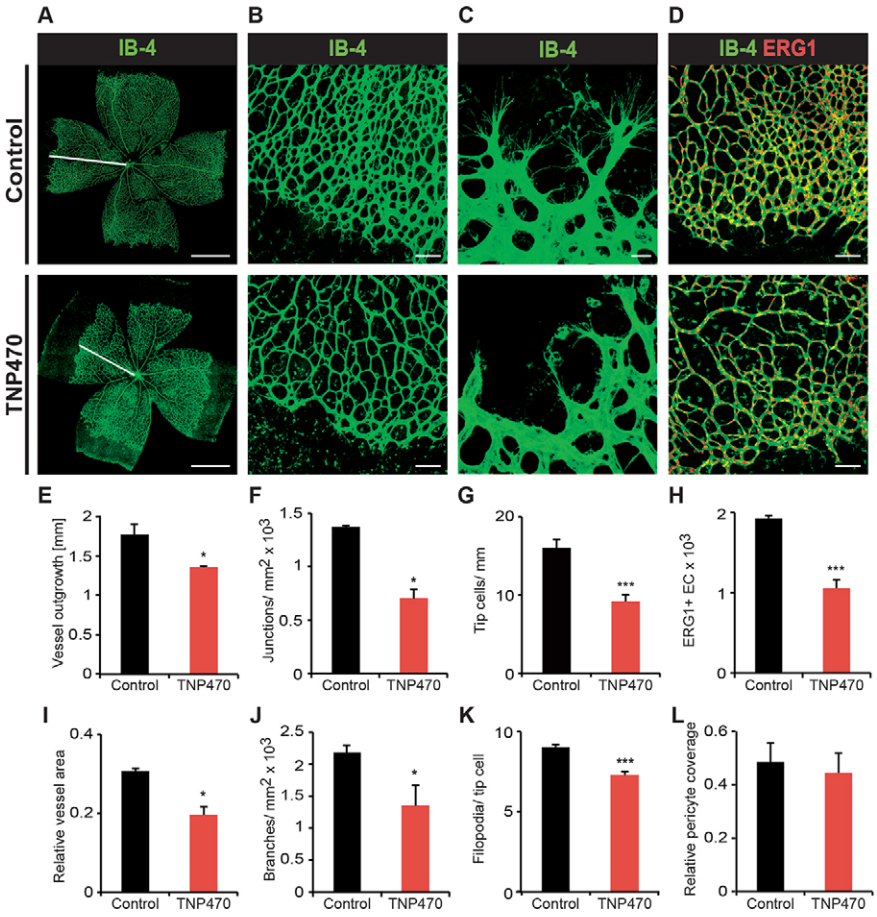

Fig. 4. Inhibition of non-canonical Wnt signaling by TNP470 treatment of mice phenocopies the reduced retina vascularization and EC number of Evi-ECKO mice. (A-C) Representative images of the total retinal vasculature (A), the sprouting front (B) and tip cells (C) stained with IB-4 in control and TNP470-treated mice. (D) Representative images of the vasculature co-stained with IB-4 and ERG1 in control and in TNP470-treated mice. (E-L) Quantifications of vessel outgrowth (E; *n*=4), junctions/mm^2 vessel area (F; *n*=4), tip cells/mm vessel front (G; *n*=5), ERG1$^+$ ECs per retina area (H; *n*=5), relative vessel area (I; *n*=4), branches/mm^2 vessel area (J; *n*=4), filopodia per tip cell (K; *n*=11) and pericyte coverage (L; *n*=14) in retinas of control and TNP-470-treated mice. Data are mean±s.d. (E,F,H-J,L) or are mean±s.e.m. (G,K). Scale bars: 1 mm (A); 100 µm (B,D); 20 µm (C). **P*<0.05, ****P*<0.001.

Evi-ECKO phenotype (Ye et al., 2010; Wang et al., 2012). Thus, EC-derived canonical Wnt ligands cannot be completely excluded from influencing vascular development. A fine-tuned interaction of canonical and non-canonical Wnt signaling might rather be important to balance the net outcome of the Wnt signaling pathways to control vessel formation. However, in the present study, the rescue of the decreased vascularization of Evi-ECKO plugs by non-canonical Wnt5a clearly demonstrated a crucial role for non-canonical Wnt ligands in controlling vessel stabilization. Other studies also support non-canonical Wnt-dependent regulation of Tek-mediated survival

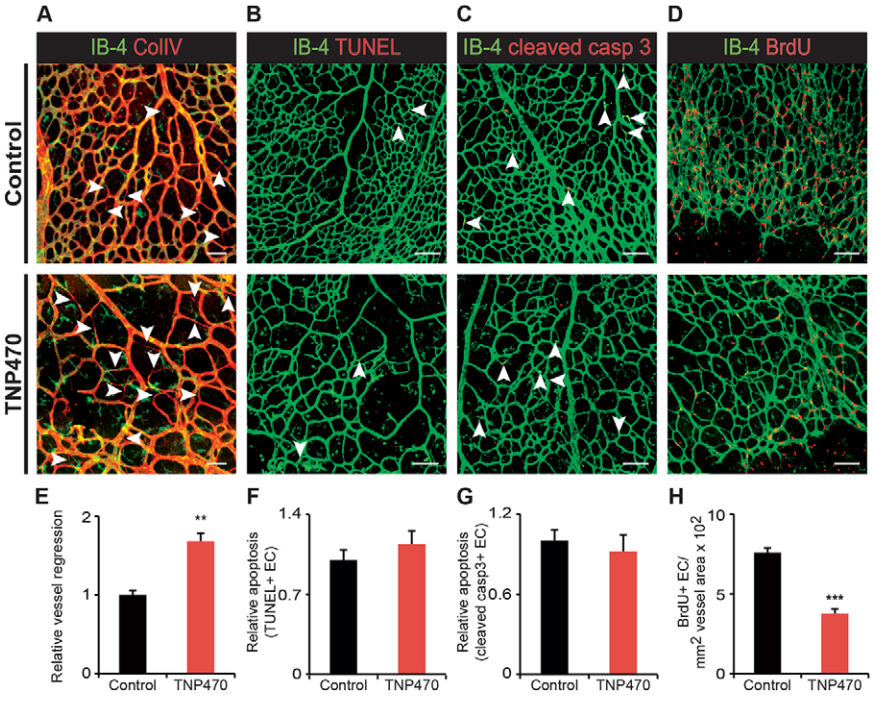

Fig. 5. Inhibition of non-canonical Wnt signaling by TNP470 treatment of mice phenocopies the remodeling phenotype of Evi-ECKO mice. (A-D) Representative images of the vasculature co-stained with IB-4 and ColIV (A), IB-4 and TUNEL (B), IB-4 and cleaved caspase-3 (C) and IB-4 and BrdU (D) in control and TNP470-treated mice. ColIV$^+$IB-4$^-$ empty sleeves, TUNEL-positive ECs and cleaved caspase-3-positive ECs are indicated by arrowheads. (E-H) Quantifications of relative vessel regression (E; *n*=4), relative TUNEL$^+$IB-4$^+$ cells per retina area (F; *n*=8), relative cleaved caspase-3$^+$IB-4$^+$ cells per retina area (G; *n*=17) and total number of BrdU$^+$IB-4$^+$ cells per retina area (H; *n*=8). Scale bars: 100 µm (B-D); 50 µm (A). Data are shown as mean±s.d. (E-H). ***P*<0.01, ****P*<0.001.

Development (2014) 141, 1757-1766 doi:10.1242/dev.104422

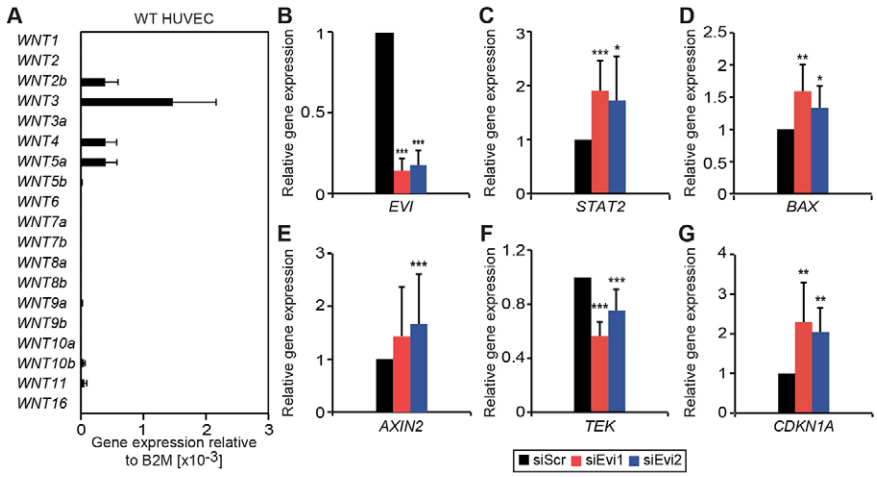

Fig. 6. Non-canonical Wnt signaling regulates survival and proliferation target gene expression in an EC-autonomous manner. (A) Wnt gene expression pattern of HUVECs. (B-G) Gene expression analysis of *EVI* (B), *STAT2* (C), *BAX* (D), *AXIN2* (E), *TEK* (F) and *CDKN1A* (G) in control-treated cells (black) and upon *EVI* silencing with two independent siRNAs (red, blue). Data are shown as mean±s.d. **P*<0.05, ***P*<0.01, ****P*<0.001.

signaling. For instance, non-canonical Wnt5a regulates TEK receptor tyrosine kinase (Tie2) expression and subsequent HUVEC survival and proliferation *in vitro* and Tek expression in lung ECs is dependent on epithelial-derived non-canonical Wnt ligands *in vivo* (Masckauchan et al., 2006; Cornett et al., 2013).

To analyze further the non-canonical Wnt-dependent regulation of vessel regression in Evi-ECKO mice, pharmacological inhibition of non-canonical Wnt signaling *in vivo* was compared with the Evi-ECKO phenotype. Treatment of mice with the non-canonical Wnt signaling inhibitor TNP470 phenocopied the reduced proliferation and increased *Cdkn1a* expression of Evi-ECKO mice, which is an important negative regulator of cell cycle progression (Zhang et al., 2000; Gartel et al., 2001; Cirone et al., 2008). Similar to the Evi-ECKO phenotype, Fgd5-dependent vessel regression correlated with increased *Cdkn1a* expression, subsequent cell cycle arrest and apoptosis, arguing for an important role of *Cdkn1a* in regulating vessel regression by interfering with EC proliferation and survival (Cheng et al., 2012). In our study, TNP470 treatment inhibited EC proliferation by promoting *Cdkn1a* upregulation, but did not affect EC apoptosis, correlating with unchanged *Tek*, *Stat2* and *Bax* expression. Thus, Tek-regulated survival signaling in Evi-ECKO mice was dependent on non-canonical, but TNP470-resistant, signaling. Wnt5a-induced *Tek* expression has previously been reported to be mediated by an Erk-dependent non-canonical pathway (Masckauchan et al., 2006). Similarly, previous studies have described TNP470-dependent induction of *Cdkn1a* expression and subsequent cell cycle arrest, which did not correlate with cytotoxic effects (Zhang et al., 2000). Along these lines, canonical Wnt signaling has been described to induce apoptosis-independent vessel regression by interfering with EC proliferation (Phng et al., 2009). Evi-ECKO mice and TNP470-treated mice both showed a reduced EC number correlating with increased vessel regression, which in the first case is due to reduced proliferation and survival and in the latter only to decreased proliferation. Therefore, we assume that a reduction in the EC number increases vessel rearrangement to adopt the vascular network in order to still provide optimal oxygen and nutrient supply to the tissue. Thus, non-canonical Wnt signaling can interfere with vessel regression by increasing EC proliferation in a TNP470-sensitive and EC survival in a TNP470-resistant manner.

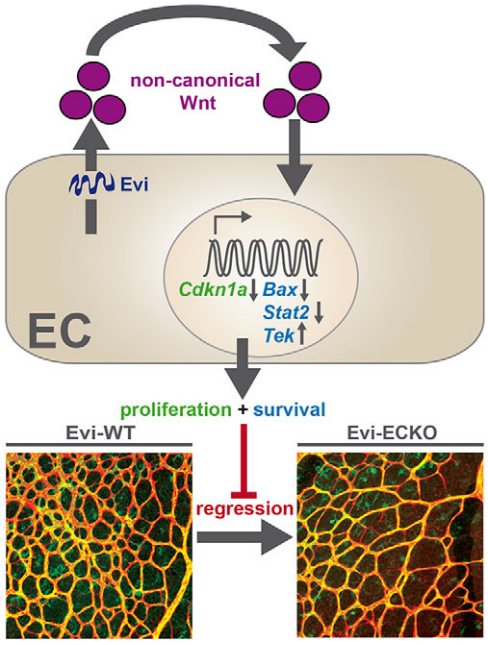

Fig. 7. Schematic of Evi-regulated vessel regression. ECs express primarily non-canonical Wnt ligands, which are secreted via Evi. Non-canonical Wnt ligands increase EC proliferation and reduce EC apoptosis via autocrine upregulation of *Tek* and inhibition of *Cdkn1a*, *Bax* and *Stat2* gene expression, thereby blocking vessel regression.

Although vessel remodeling was affected in Evi-ECKO mice, EC sprouting and stabilization by pericytes was not altered. TNP470 treatment similarly did not affect pericyte coverage, but interfered with EC sprouting as indicated by reduced filopodia formation. PCP signaling has been linked to downstream activation of small GTPases, such as Rho and Rac, which have been shown to be important for VEGF-induced vessel sprouting (De Smet et al., 2009). TNP470 interferes with VEGF-dependent activation of these GTPases in HUVECs, thereby preventing VEGF-induced cell-cell adhesion, migration and cytoskeletal rearrangements (Satchi-Fainaro et al., 2005; Nahari et al., 2007). Hence, besides affecting proliferation in a *Cdkn1a*-dependent manner, TNP470 might inhibit sprouting by interfering with Rho and Rac1 signaling independently of EC-derived Wnt ligands.

Several cell types of the vascular system, including ECs, pericytes, astrocytes, neural cells and macrophages, secrete Wnt ligands, which contribute to the regulation of EC functions during vessel remodeling. For example, macrophage-derived Wnt5a interferes with retinal vessel formation and, similarly, glia cells inhibit canonical Wnt signaling in ECs and subsequent vessel regression (Stefater et al., 2011; Ma et al., 2013). We analyzed in the present

Development (2014) 141, 1757-1766 doi:10.1242/dev.104422

study the contribution of EC-derived Wnt ligands in controlling vessel remodeling. Owing to the presence of bystander cells *in vivo*, it cannot be excluded that vessel remodeling in Evi-ECKO mice was exclusively regulated in an EC-autonomous manner. However, cultured HUVECs showed similar gene regulation of *BAX*, *TEK*, *STAT2* and *CDKN1A* upon *EVI* silencing in the absence of any bystander cells, arguing for a primarily EC-autonomous regulation of vascular remodeling. Furthermore, blood vessel density was reduced in the retina and in LLC tumors upon *Evi* deletion, also arguing for control of vessel stabilization by EC-derived Wnt ligands that is independent of different environmental Wnt sources.

In summary, the identification of EC-derived non-canonical Wnt ligands as novel regulators of vessel remodeling is of major impact for the molecular understanding of the processes regulating physiological vessel regression and vascular pruning. As such, a better understanding of the molecular mechanisms of vessel remodeling may well pave the way to improve therapeutic targeting of pathological angiogenesis.

MATERIALS AND METHODS

Mice

Floxed *Evi* mice (*Evi*$^{fl/fl}$) were generated as described previously (Augustin et al., 2013). Briefly, the *Evi* locus was targeted by flanking exon 3 of the *Evi* gene by loxP sites. *Evi*$^{fl/fl}$ mice were crossed to *Tg(Cdh5-cre/ERT2)1Rha (Cdh5CreERT2)* mice (Wang et al., 2010) to specifically delete exon 3 and, thus, *Evi* gene expression in ECs. Genotyping of the *Evi* wild-type and mutant allele and the *Cdh5CreERT2* allele was carried out by PCR with the indicated primers (supplementary material Table S1). To induce *Evi* deletion in mouse pups, mice were intra-gastrically (i.g.) injected with 100 µg tamoxifen (Sigma, T5648) in 50 µl peanut oil/5% ethanol at P1, P2 and P3. For TNP470 treatment, C57/Bl6 mice were injected with 50 mg/kg TNP470 (Sigma, T1455) in ethanol/0.9% NaCl s.c. at P1-P5 and retinas were isolated at P6 or in case of apoptosis analysis 4 h after the last injection. Control-treated animals were injected with the same amount of ethanol/0.9% NaCl. Mice were housed in individually ventilated cages under pathogen-free conditions. Animals had free access to food and water and were kept in a 12-h light-dark cycle. Mutant and control littermates were used for all experiments. All animal experiments were approved by the local regulatory committee (Bezirksregierung Karlsruhe, Germany; permit #G107/12).

Tumor cell implantation

For tumor experiments, 6-week-old Evi-ECKO and control mice were injected with 10^6 LLC cells s.c. To induce *Evi* deletion, mice were intraperitoneally (i.p.) injected with 2 mg tamoxifen (Sigma, T5648) in 100 µl peanut oil 2, 4, 6, 8 and 11 days after tumor cell injection. Tumors were harvested after 13 days and embedded in Tissue-Tek OCT compound.

Retinal whole-mount staining

At P6, mice were sacrificed, eyeballs were isolated and fixed in either ice-cold methanol or 4% paraformaldehyde (PFA). Retinas were isolated and blocking was performed with 0.5% Triton X-100/1% bovine serum albumin/10% goat serum in PBS for 1 h at room temperature (RT). The retina vasculature was stained with FITC-conjugated Isolectin B-4 (IB-4, Sigma L9381; 1:100) and the denoted primary antibodies (supplementary material Table S2) overnight at 4°C and subsequently incubated with the appropriate secondary antibodies for 1 h at RT. For TUNEL staining, 4% PFA-fixed retinas were permeabilized with 0.5% Triton X-100/0.1% citrate for 3 h at RT and subsequently stained with the In Situ Cell Death Detection Kit according to the manufacturer's protocol (Roche, 2156792). Afterwards, the retinal vasculature was visualized by staining with IB-4 for 1 h at RT. Pictures were taken with the confocal microscopes Zeiss LSM700 and Zeiss LSM710 and image analysis was accomplished with Fiji (ImageJ). The relative vessel area was calculated as IB-4$^+$ area per retina area. Junctions and branches were counted in eight individual 600 µm×600 µm fields of comparable regions in the retina and normalized to the vessel area. For tip cell analysis, the number of tip cells at the total retina front was determined and depicted as tip cells per mm vessel front. Furthermore, the number of filopodia per tip cell was analyzed in ten pictures per retina. For the analysis of EC apoptosis, TUNEL$^+$ and cleaved caspase3$^+$ structures that colocalized with IB-4 staining were counted and correlated to the vessel area. Pericyte coverage was determined by measuring the desmin$^+$ area associated with the vasculature and correlating it to the vessel area. Erg-1$^+$ cells were normalized to the retina area. Regression analysis was accomplished by counting ColIV$^+$IB-4$^-$ structures and correlating them to the vessel area. If depicted as relative value, the single values per mouse were normalized to the average of the littermate WT or control-treated animals. Each litter was analyzed separately.

BrdU labeling *in vivo*

For analysis of proliferation, mice were injected s.c. with BrdU (50 µg/g mouse) 3 h prior to sacrificing the animals. Eyes were removed and fixed in ice-cold methanol. Retinas were isolated and incubated with 2 N HCl/0.5% Triton X-100 for 1 h at 37°C. Retinas were washed three times with 0.1 M $B_4Na_2O_7{\cdot}10H_2O$ for 10 min, subsequently blocked and stained for BrdU with the annotated antibody (supplementary material Table S1) as described in the previous section. BrdU$^+$IB4$^+$ nuclei were counted and normalized to the vessel area in 600 µm×600 µm regions of the proliferating front. Six regions were analyzed per retina.

Matrigel plug assay

Geltrex LDEV-free reduced growth factor basement membrane matrix (400 µl) (Gibco) was mixed with 500 ng bFGF (R&D, 3139-FB-025/CF) in 100 µl PBS or 500 ng bFGF and 500 ng Wnt5a (R&D, 654-WN-010/CF) in 100 µl PBS. Matrigel plugs were implanted s.c. into 6-week-old Evi-ECKO and littermate WT mice. To induce *Evi* deletion, mice were intraperitoneally (i.p.) injected with 2 mg tamoxifen (Sigma, T5648) in 100 µl peanut oil 1, 2, 4, 5 and 7 days after Matrigel plug implantation. Plugs were excised after 8 days, fixed in zinc fixative [3 mM $Ca(C_2H_3O_2)_2$, 2.2 mM $Zn(C_2H_3O_2)_2$, 3.6 mM $ZnCl_2$, 0.1 M Tris] and embedded in paraffin. Paraffin sections (6 µm) were prepared and three sections of three different plug regions were used for analysis.

Immunofluorescence staining

Tumor cryosections were fixed in ice-cold methanol for 10 min at −20°C. Paraffin sections were deparaffinized in xylene and passed though graded alcohols. Antigen-retrieval was performed with 8 µg/ml Proteinase K in Tris-EDTA (TE) buffer (10 mM Tris, 1 mM EDTA, pH 8.0) for 10 min at 37°C. Cryosections and paraffin-embedded sections were blocked with 10% normal goat serum (Life Technologies) for 1 h at RT. The vasculature was stained for CD31 for 1 h at RT or overnight at 4°C for cryosections and paraffin-embedded sections, respectively (supplementary material Table S2). The sections were subsequently incubated with the appropriate secondary antibody for 1 h at RT (supplementary material Table S2). Pictures were taken using the Zeiss Cell Observer and image analysis was accomplished with Fiji. The number of vessels and the vessel area were correlated to the tumor area or Matrigel-plug area.

Lung and retina EC sorting by FACS

Mice were sacrificed and lungs of single P6 or adult mice were surgically removed and cut into small pieces. For isolation of ECs from retinas of adult or P6 mice, ten mice were pooled and retinas were homogenized by passing through a 1 ml pipette. Subsequently, retinas and lungs were digested with Dulbecco's Modified Eagle's medium (DMEM) containing 1.25 mM $CaCl_2$, 200 U/ml Collagenase I and 10 µg/ml DnaseI at 37°C for 15 min and 45 min, respectively. Single-cell suspensions of the digested organs were prepared by passing them through 18 G and 19 G cannula syringes and filtering the lysates through a 100 µm cell strainer. Cells were stained for the negative markers podoplanin (Pdpn), Lyve1, CD45 (also known as Ptprc) and Ter119 (also known as Ly76) with the antibodies listed (supplementary material Table S2) for 30 min at 4°C in PBS/5% fetal calf serum (FCS). Negatively stained cells were depleted by incubating them with 500 µl Dynabeads magnetic beads (Life Technologies) in 750 µl PBS/5% FCS for 30 min at 4°C on the rotator. The remaining cells were positively stained with antibodies against CD31 and CD34 (supplementary material Table S2) in PBS/5% FCS for 30 min at 4°C.

Development (2014) 141, 1757-1766 doi:10.1242/dev.104422

Dead cells were excluded by phosphatidylinositol (PI) staining (1:3000). $CD45^-Ter119^-Lyve1^-Pdpn^-PI^-CD31^+CD34^+$ cells were sorted in the case of lung ECs and $CD45^-Ter119^-PI^-CD31^+CD34^+$ cells in the case of retinal ECs with a BD Biosciences FACSAria Cell Sorter [German Cancer Research Center (DKFZ) core facility].

RNA isolation and real-time quantitative PCR (RT-qPCR) analysis

RNA of FACS-sorted mouse ECs was isolated with Arcturus PicoPure RNA Isolation Kit (Life Technologies) and RNA of HUVECs was isolated with RNeasy Mini Kit (Qiagen) according to the manufacturer's protocols. cDNA was synthesized with QuantiTect Reverse Transcription Kit (Qiagen) according to the manufacturer's instructions. Subsequent (RT)-qPCR was performed with TaqMan gene expression assay (Life Technologies; see supplementary material Table S3), TaqMan Fast Advanced Mastermix (Life Technologies) and Roche Light Cycler 480. TaqMan probes are annotated in supplementary material Table S3. In case of human *BAX* and *AXIN2* expression, (RT)-qPCR was performed with Power SYBRGreen PCR Master Mix (Applied Biosystems) using the listed primer sequences (supplementary material Table S1).

Cell culture

Lewis lung carcinoma cells were cultured at 37°C in DMEM with 10% FCS in 5% CO_2 and high humidity. HUVECs were cultured in Endopan with 3% FCS and supplements (PAN Biotech) in 5% CO_2 and high humidity. For *EVI* silencing in HUVECs, 1.2×10^5 cells were seeded. After 24 h, cells were transfected with 200 nM Silencer select Evi siRNA or control siRNA (Life Technologies) using 5 µl Oligofectamin (Life Technologies, 12252-011) in 1 ml Opti-MEM I(1×)+GlutaMAX-I (Life Technologies, 51985-026). The medium was changed to Endopan with 3% FCS and supplements after 4 h and gene expression was analyzed after 48 h.

Statistical analysis

Statistical analysis was performed using Sigma-Plot (Systat Software). Unless otherwise stated, data are expressed as mean±s.d. Statistical significance was determined by two-tailed Student's *t*-test. In the Matrigel plug assay, multiple group comparison was performed with an ANOVA followed by Bonferroni's post-hoc correction. A *P*-value of less than 0.05 was considered statistically significant and marked by asterisks (*P<0.05, **P<0.01, ***P<0.001). *n* represents the number of independent mice analyzed per group.

Acknowledgements

We thank the excellent technical support by the DKFZ laboratory animal, imaging and FACS core facilities.

Competing interests

The authors declare no competing financial interests.

Author contributions

C.K. and B.S. designed and performed research, analyzed and interpreted data, and wrote the manuscript; J.H. and K.S. performed research; J.W. and T.A. collected data; R.H.A. provided mice; M.B., H.G.A. and I.A. designed and conceptualized research, analyzed and interpreted data, and wrote the manuscript.

Funding

This work was supported by grants from the Deutsche Forschungsgemeinschaft [SFB873 'Stem Cells in Development and Disease' to H.G.A. and M.B.; SFB-TR23 'Vascular Differentiation and Remodeling' to H.G.A.]; a German Cancer Research Center (DKFZ) intramural collaboration grant (to H.G.A. and M.B.); the European Union FP7 program 'SyStemAge' (to H.G.A.); and the Leducq Foundation (to H.G.A.). H.G.A. is supported by an endowed chair from the Aventis Foundation.

Supplementary material

Supplementary material available online at
http://dev.biologists.org/lookup/suppl/doi:10.1242/dev.104422/-/DC1

References

Alon, T., Hemo, I., Itin, A., Pe'er, J., Stone, J. and Keshet, E. (1995). Vascular endothelial growth factor acts as a survival factor for newly formed retinal vessels and has implications for retinopathy of prematurity. *Nat. Med.* **1**, 1024-1028.

Augustin, H. G., Koh, G. Y., Thurston, G. and Alitalo, K. (2009). Control of vascular morphogenesis and homeostasis through the angiopoietin-Tie system. *Nat. Rev. Mol. Cell Biol.* **10**, 165-177.

Augustin, I., Gross, J., Baumann, D., Korn, C., Kerr, G., Grigoryan, T., Mauch, C., Birchmeier, W. and Boutros, M. (2013). Loss of epidermal Evi/Wls results in a phenotype resembling psoriasiform dermatitis. *J. Exp. Med.* **210**, 1761-1777.

Baffert, F., Le, T., Sennino, B., Thurston, G., Kuo, C. J., Hu-Lowe, D. and McDonald, D. M. (2006). Cellular changes in normal blood capillaries undergoing regression after inhibition of VEGF signaling. *Am. J. Physiol. Heart Circ. Physiol.* **290**, H547-H559.

Bartscherer, K., Pelte, N., Ingelfinger, D. and Boutros, M. (2006). Secretion of Wnt ligands requires Evi, a conserved transmembrane protein. *Cell* **125**, 523-533.

Cattelino, A., Liebner, S., Gallini, R., Zanetti, A., Balconi, G., Corsi, A., Bianco, P., Wolburg, H., Moore, R., Oreda, B. et al. (2003). The conditional inactivation of the beta-catenin gene in endothelial cells causes a defective vascular pattern and increased vascular fragility. *J. Cell Biol.* **162**, 1111-1122.

Cheng, C., Haasdijk, R., Tempel, D., van de Kamp, E. H., Herpers, R., Bos, F., Den Dekker, W. K., Blonden, L. A. J., de Jong, R., Burgisser, P. E. et al. (2012). Endothelial cell-specific FGD5 involvement in vascular pruning defines neovessel fate in mice. *Circulation* **125**, 3142-3159.

Cirone, P., Lin, S., Griesbach, H. L., Zhang, Y., Slusarski, D. C. and Crews, C. M. (2008). A role for planar cell polarity signaling in angiogenesis. *Angiogenesis* **11**, 347-360.

Clevers, H. and Nusse, R. (2012). Wnt/beta-catenin signaling and disease. *Cell* **149**, 1192-1205.

Corada, M., Nyqvist, D., Orsenigo, F., Caprini, A., Giampietro, C., Taketo, M. M., Iruela-Arispe, M. L., Adams, R. H. and Dejana, E. (2010). The Wnt/beta-catenin pathway modulates vascular remodeling and specification by upregulating Dll4/Notch signaling. *Dev. Cell* **18**, 938-949.

Cornett, B., Snowball, J., Varisco, B. M., Lang, R., Whitsett, J. and Sinner, D. (2013). Wntless is required for peripheral lung differentiation and pulmonary vascular development. *Dev. Biol.* **379**, 38-52.

Daneman, R., Agalliu, D., Zhou, L., Kuhnert, F., Kuo, C. J. and Barres, B. A. (2009). Wnt/beta-catenin signaling is required for CNS, but not non-CNS, angiogenesis. *Proc. Natl. Acad. Sci. U.S.A.* **106**, 641-646.

De Smet, F., Segura, I., De Bock, K., Hohensinner, P. J. and Carmeliet, P. (2009). Mechanisms of vessel branching: filopodia on endothelial tip cells lead the way. *Arterioscler. Thromb. Vasc. Biol.* **29**, 639-649.

Descamps, B., Sewduth, R., Ferreira Tojais, N., Jaspard, B., Reynaud, A., Sohet, F., Lacolley, P., Allieres, C., Lamaziere, J.-M. D., Moreau, C. et al. (2012). Frizzled 4 regulates arterial network organization through noncanonical Wnt/planar cell polarity signaling. *Circ. Res.* **110**, 47-58.

Gartel, A. L., Ye, X., Goufman, E., Shianov, P., Hay, N., Najmabadi, F. and Tyner, A. L. (2001). Myc represses the p21(WAF1/CIP1) promoter and interacts with Sp1/Sp3. *Proc. Natl. Acad. Sci. U.S.A.* **98**, 4510-4515.

Goodwin, A. M., Sullivan, K. M. and D'Amore, P. A. (2006). Cultured endothelial cells display endogenous activation of the canonical Wnt signaling pathway and express multiple ligands, receptors, and secreted modulators of Wnt signaling. *Dev. Dyn.* **235**, 3110-3120.

Ingber, D., Fujita, T., Kishimoto, S., Sudo, K., Kanamaru, T., Brem, H. and Folkman, J. (1990). Synthetic analogues of fumagillin that inhibit angiogenesis and suppress tumour growth. *Nature* **348**, 555-557.

Ishida, S., Yamashiro, K., Usui, T., Kaji, Y., Ogura, Y., Hida, T., Honda, Y., Oguchi, Y. and Adamis, A. P. (2003). Leukocytes mediate retinal vascular remodeling during development and vaso-obliteration in disease. *Nat. Med.* **9**, 781-788.

Kim, H. S. and Lee, M.-S. (2007). STAT1 as a key modulator of cell death. *Cell. Signal.* **19**, 454-465.

Liebner, S., Corada, M., Bangsow, T., Babbage, J., Taddei, A., Czupalla, C. J., Reis, M., Felici, A., Wolburg, H., Fruttiger, M. et al. (2008). Wnt/beta-catenin signaling controls development of the blood-brain barrier. *J. Cell Biol.* **183**, 409-417.

Lobov, I. B., Cheung, E., Wudali, R., Cao, J., Halasz, G., Wei, Y., Economides, A., Lin, H. C., Papadopoulos, N., Yancopoulos, G. D. et al. (2011). The Dll4/Notch pathway controls postangiogenic blood vessel remodeling and regression by modulating vasoconstriction and blood flow. *Blood* **117**, 6728-6737.

Ma, S., Kwon, H. J., Johng, H., Zang, K. and Huang, Z. (2013). Radial glial neural progenitors regulate nascent brain vascular network stabilization via inhibition of Wnt signaling. *PLoS Biol.* **11**, e1001469.

Martinou, J. C. and Youle, R. J. (2011). Mitochondria in apoptosis: Bcl-2 family members and mitochondrial dynamics. *Dev. Cell* **21**, 92-101.

Masckauchan, T. N. H., Agalliu, D., Vorontchikhina, M., Ahn, A., Parmalee, N. L., Li, C.-M., Khoo, A., Tycko, B., Brown, A. M. C. and Kitajewski, J. (2006). Wnt5a signaling induces proliferation and survival of endothelial cells in vitro and expression of MMP-1 and Tie-2. *Mol. Biol. Cell* **17**, 5163-5172.

Nahari, D., Satchi-Fainaro, R., Chen, M., Mitchell, I., Task, L. B., Liu, Z., Kihneman, J., Carroll, A. B., Terada, L. S. and Nwariaku, F. E. (2007). Tumor cytotoxicity and endothelial Rac inhibition induced by TNP-470 in anaplastic thyroid cancer. *Mol. Cancer Ther.* **6**, 1329-1337.

Phng, L.-K., Potente, M., Leslie, J. D., Babbage, J., Nyqvist, D., Lobov, I., Ondr, J. K., Rao, S., Lang, R. A., Thurston, G. et al. (2009). Nrarp

Development (2014) 141, 1757-1766 doi:10.1242/dev.104422

coordinates endothelial Notch and Wnt signaling to control vessel density in angiogenesis. *Dev. Cell* **16**, 70-82.

Potente, M., Gerhardt, H. and Carmeliet, P. (2011). Basic and therapeutic aspects of angiogenesis. *Cell* **146**, 873-887.

Rao, S., Lobov, I. B., Vallance, J. E., Tsujikawa, K., Shiojima, I., Akunuru, S., Walsh, K., Benjamin, L. E. and Lang, R. A. (2007). Obligatory participation of macrophages in an angiopoietin 2-mediated cell death switch. *Development* **134**, 4449-4458.

Reis, M., Czupalla, C. J., Ziegler, N., Devraj, K., Zinke, J., Seidel, S., Heck, R., Thom, S., Macas, J., Bockamp, E. et al. (2012). Endothelial Wnt/beta-catenin signaling inhibits glioma angiogenesis and normalizes tumor blood vessels by inducing PDGF-B expression. *J. Exp. Med.* **209**, 1611-1627.

Satchi-Fainaro, R., Mamluk, R., Wang, L., Short, S. M., Nagy, J. A., Feng, D., Dvorak, A. M., Dvorak, H. F., Puder, M., Mukhopadhyay, D. et al. (2005). Inhibition of vessel permeability by TNP-470 and its polymer conjugate, caplostatin. *Cancer Cell* **7**, 251-261.

Stefater, J. A., III, Lewkowich, I., Rao, S., Mariggi, G., Carpenter, A. C., Burr, A. R., Fan, J., Ajima, R., Molkentin, J. D., Williams, B. O. et al. (2011). Regulation of angiogenesis by a non-canonical Wnt-Flt1 pathway in myeloid cells. *Nature* **474**, 511-515.

Stefater, J. A., III, Rao, S., Bezold, K., Aplin, A. C., Nicosia, R. F., Pollard, J. W., Ferrara, N. and Lang, R. A. (2013). Macrophage Wnt-Calcineurin-Flt1 signaling regulates mouse wound angiogenesis and repair. *Blood* **121**, 2574-2578.

Stenman, J. M., Rajagopal, J., Carroll, T. J., Ishibashi, M., McMahon, J. and McMahon, A. P. (2008). Canonical Wnt signaling regulates organ-specific assembly and differentiation of CNS vasculature. *Science* **322**, 1247-1250.

Wang, H., Charles, P. C., Wu, Y., Ren, R., Pi, X., Moser, M., Barshishat-Kupper, M., Rubin, J. S., Perou, C., Bautch, V. et al. (2006). Gene expression profile signatures indicate a role for Wnt signaling in endothelial commitment from embryonic stem cells. *Circ. Res.* **98**, 1331-1339.

Wang, Y., Nakayama, M., Pitulescu, M. E., Schmidt, T. S., Bochenek, M. L., Sakakibara, A., Adams, S., Davy, A., Deutsch, U., Lüthi, U. et al. (2010). Ephrin-B2 controls VEGF-induced angiogenesis and lymphangiogenesis. *Nature* **465**, 483-486.

Wang, Y., Rattner, A., Zhou, Y., Williams, J., Smallwood, P. M. and Nathans, J. (2012). Norrin/Frizzled4 signaling in retinal vascular development and blood brain barrier plasticity. *Cell* **151**, 1332-1344.

Ye, X., Wang, Y., Cahill, H., Yu, M., Badea, T. C., Smallwood, P. M., Peachey, N. S. and Nathans, J. (2010). Norrin, Frizzled-4, and Lrp5 signaling in endothelial cells controls a genetic program for retinal vascularization. *Cell* **141**, 191.

Zhang, Y., Griffith, E. C., Sage, J., Jacks, T. and Liu, J. O. (2000). Cell cycle inhibition by the anti-angiogenic agent TNP-470 is mediated by p53 and p21 (WAF1/CIP1). *Proc. Natl. Acad. Sci. U.S.A.* **97**, 6427-6432.

Zhang, Y., Yeh, J. R., Mara, A., Ju, R., Hines, J. F., Cirone, P., Griesbach, H. L., Schneider, I., Slusarski, D. C., Holley, S. A. et al. (2006). A chemical and genetic approach to the mode of action of fumagillin. *Chem. Biol.* **13**, 1001-1009.

Supplemental Figures

Korn et al. Figure S1

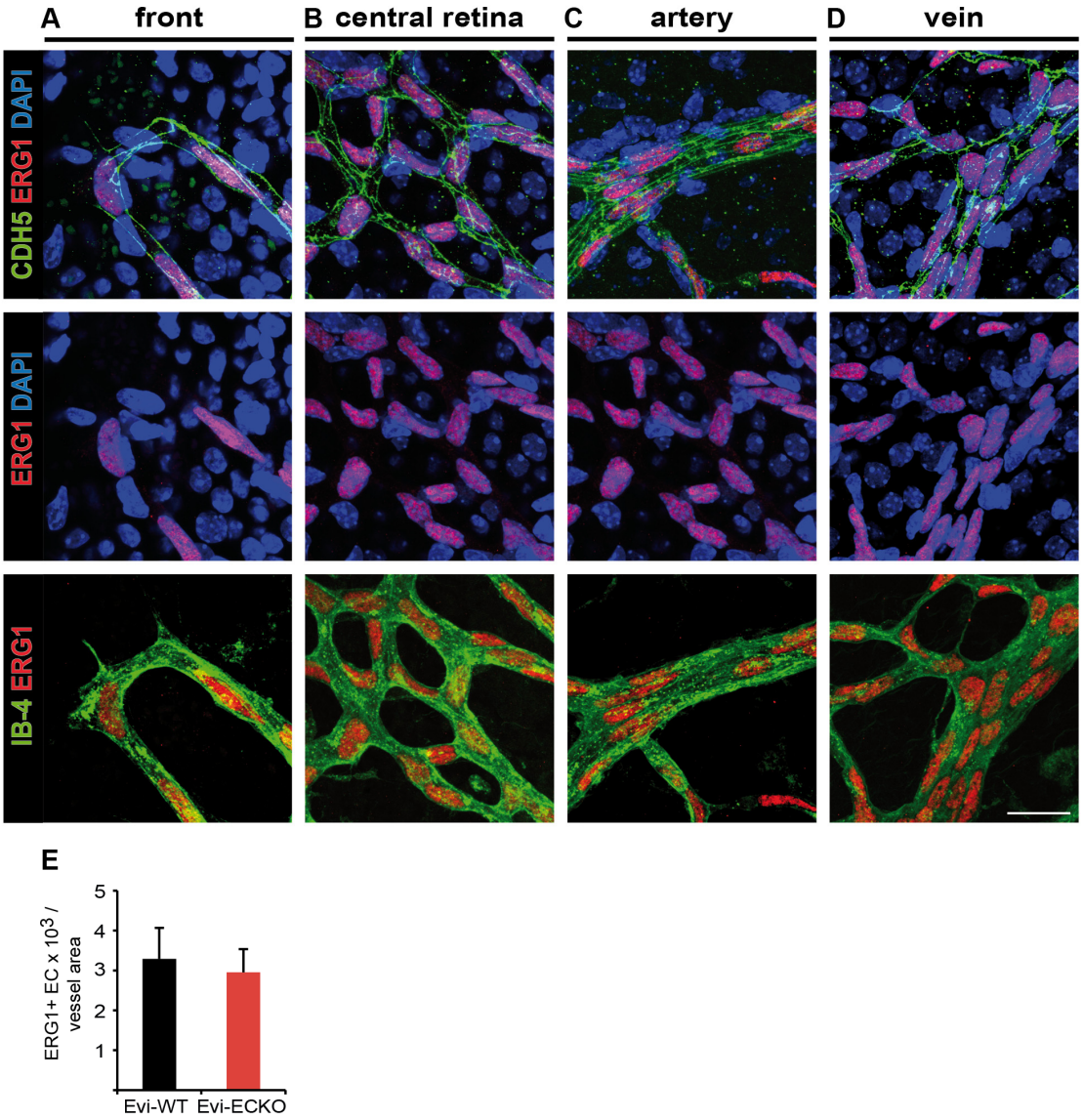

Fig. S1 ERG1 staining in the mouse retina for EC labeling. Representative images in different regions of the retina including vascular front (A), central retina (B), artery (C) and vein (D) co-stained for CDH5, ERG1 and DAPI (upper row), for ERG1 and DAPI (middle row) or for IB-4 and ERG-1 (lower row). Quantifications of ERG1$^+$ EC per IB-4 stained vessel area (E, n=17) reveals a linear correlation between vessel area and ERG1$^+$ EC number further supporting a uniform ERG1 expression throughout the retinal vasculature. Scale bar 20 µm. Data is shown as mean±s.d.

Korn et al. Figure S2

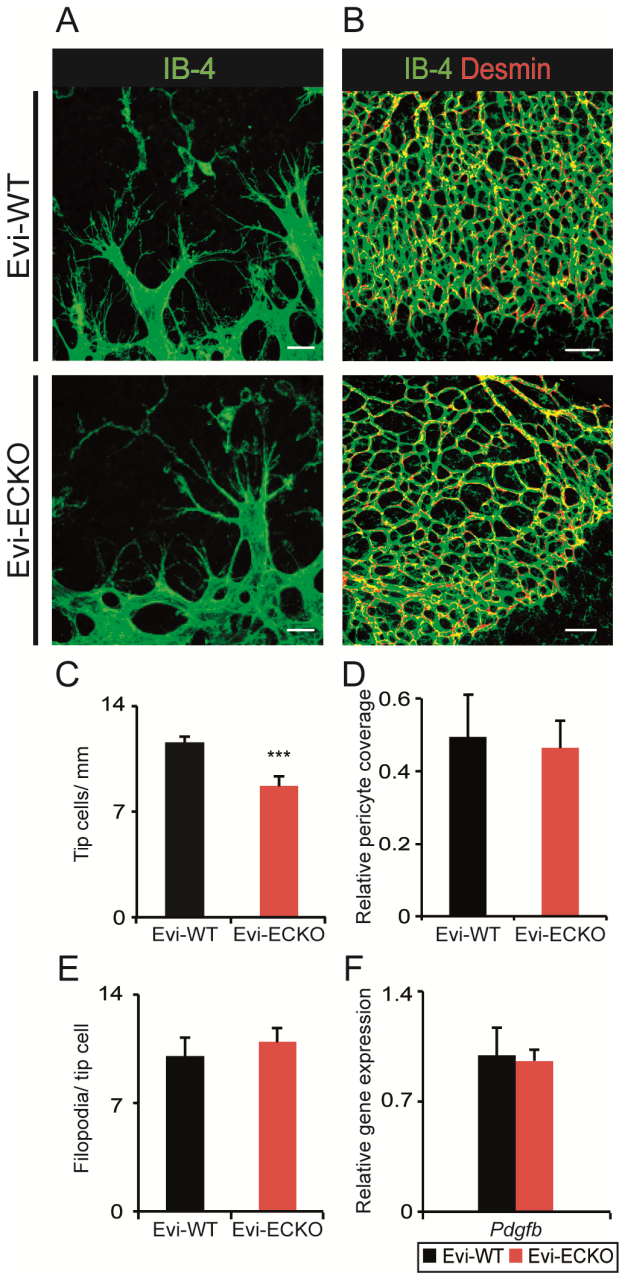

Fig. S2 Vessel sprouting and maturation are not affected in Evi-ECKO mice. Representative images of tip cells stained with IB-4 in (A). Representative images of the vasculature co-stained with IB-4 and desmin in Evi-WT and Evi-ECKO mice (B). Quantifications of tip cells/mm vessel front (C; n=16), pericytes coverage (D; n=10), filopodia per tip cell (E; n=6) and *Pdgfb* gene expression analysis of FACS sorted lung EC (F). Scale bar, 20 µm (A) and 100µm (B). Data are shown as mean±s.d. (D-F) or mean± s.e.m. (C).***P<0.001

Korn et al. Figure S3

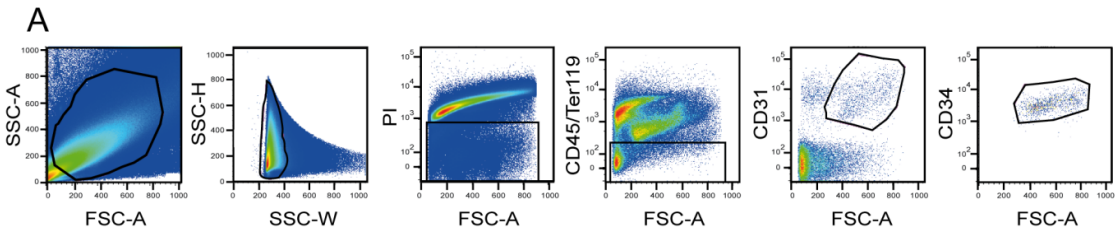

Fig. S3 FACS sorting scheme for the isolation of EC from mouse retina. Representative FACS sorting scheme for the isolation of retinal EC. $CD45^{-}Ter119^{-}PI^{-}CD31^{+}CD34^{+}$ cells were sorted for EC gene expression analysis.

Korn et al. Figure S4

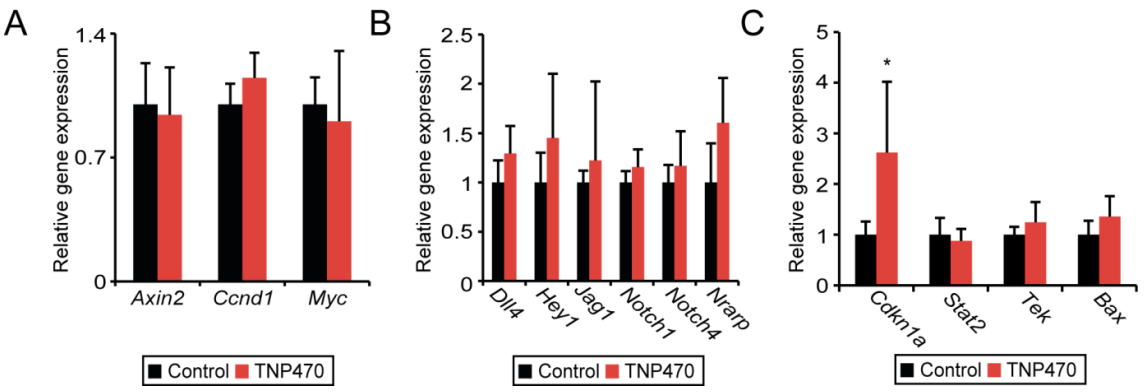

Fig. S4 Target gene expression upon TNP470 treatment. Gene expression analyses of canonical target genes (A), Notch genes (B) as well as survival and proliferation related genes (C) in lung EC of control (black) and TNP470-treated (red) mice. Data are shown as mean±s.d. *P<0.05

Korn et al. Figure S5

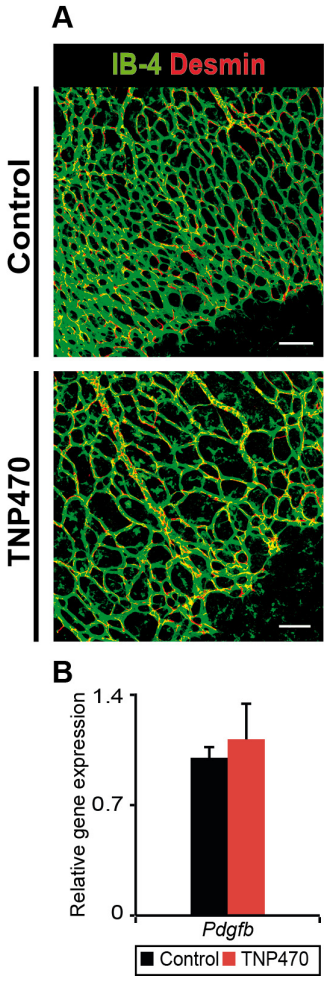

Fig. S5 Pericyte coverage is similar upon TNP470 treatment. Representative images of the vasculature co-stained with IB-4 and desmin in control- and TNP470-treated animals (A). *Pdgfb* gene expression analysis in control- and TNP470-treated (B) animals. Scale bar 100µm. Data are shown as mean±s.d.

Table S1: Primers

primer	sequence 5'-3'	method
CdhCreERT2 fwd	gcctgcattaccggtcgatgcaacga	genotyping PCR
CdhCreERT2 rev	gtggcagatggcgcggcaacaccatt	genotyping PCR
Evi fwd	aaggaaacgagattgagatgagg	genotyping PCR
Evi rev	gtttatttttcctcttaccactctg	genotyping PCR
human *Axin2* fwd	tgacggatgattccatgtcc	(RT)-qPCR
human *Axin2* rev	gttccacgggggtcatctc	(RT)-qPCR
human *Bax* fwd	catggagctgcagaggatgat	(RT)-qPCR
human *Bax* rev	gtcagctgccactcggaaaa	(RT)-qPCR
human *Gapdh* fwd	agcctcccgcttcgctctct	(RT)-qPCR
human *Gapdh* rev	ccaggcgcccaatacgacca	(RT)-qPCR

Table S2: Antibodies

antibody	reactivity	species	dilution	Conjugate	company	catalog number
BrdU		mouse	1:100	-	Roche	11170376001
Cadherin-5	Mouse	rat	1:300		BD Pharmingen	550548
CD31	mouse	rat	1:100	APC	BD Pharmingen	551262
CD31	mouse	rat	1:100	-	BD	553370
CD34	mouse	rat	1:50	Pacific Blue	BD Pharmingen	560230
CD45	mouse	rat	1:400	FITC	BD Pharmingen	553080
Cleaved caspase 3	mouse	rabbit	1:300	-	Cell signaling	9661
Collagen IV	mouse	rabbit	1:100	-	Serotec	2150-1470
Desmin	mouse	rabbit	1:100	-	Abcam	Ab15200-1
ERG1	mouse	rabbit	1:100	-	Abcam	ab92513
Lyve-1	mouse	rat	1:250	FITC	eBioscience	53-0443
Podoplanin	mouse	hamster	1:100	Alexa488	eBioscience	53-5381
Ter119	mouse	rat	1:200	FITC	BD Pharmingen	561032
IgG	rabbit	goat	1:500	Alexa546	Invitrogen	A11071
IgG	rat	goat	1:500	Alexa488	Invitrogen	A11081
IgG	mouse	goat	1:500	Alexa546	Invitrogen	A11003

Table S3: TaqMan probes

mouse probes	ordering number	human probes	ordering number
mouse *Actin*	Mm00607939_S1	human *AXIN2*	Hs00610344_m1
mouse *Agt*	Mm00599662_m1	human *B2M*	Hs00984230_m1
mouse *Axin2*	Mm00443610_m1	human *CDKN1A*	Hs00355782_m1
mouse *b2m*	Mm00437762_m1	human *EVI*	Hs01553062_m1
mouse *Bax*	Mm00432051_m1	human *GAPDH*	Hs02758991_g1
mouse *Ccnd1*	Mm00432359_m1	human STAT2	Hs01013123_m1
mouse *Cdkn1a*	Mm04205640_g1	human *TEK*	Hs00945146_m1
mouse *Dll4*	Mm00444619_m1	human *WNT1*	Hs01011247_m1
mouse *Ednra*	Mm01243722_m1	human *WNT10a*	Hs00228741_m1
mouse *Evi*	Mm00509695_m1	human *WNT10a*	Hs00228741_m1
mouse *Hey1*	Mm00468865_m1	human *WNT10b*	Hs00559664_m1
mouse *Hey2*	Mm00469280_m1	human *WNT11*	Hs00182986_m1
mouse *Jag1*	Mm00496902_m1	human *WNT16*	Hs00365138_m1
mouse *Myc*	Mm00487804_m1	human *WNT2*	Hs00608224_m1
mouse *Notch1*	Mm00435249_m1	human *WNT2b*	Hs00921614_m1
mouse *Notch4*	Mm00440525_m1	human *WNT3*	Hs00902257_m1
mouse *Nrarp*	Mm00482529_s1	human *WNT3a*	Hs00263977_m1
mouse *Pdgfb*	Mm00440677_m1	human *WNT4*	Hs01573504_m1
mouse *Stat2*	Mm00490880_m1	human *WNT5a*	Hs00998537_m1
mouse *Tek*	Mm00443254_m1	human *WNT5b*	Hs01086864_m1
mouse *Vegfa*	Mm01281449_m1	human *WNT6*	Hs00362452_m1
mouse *Wnt1*	Mm01300555_g1	human *WNT7a*	Hs01114990_m1
mouse *Wnt10a*	Mm00437325_m1	human *WNT7b*	Hs00536497_m1
mouse *Wnt10b*	Mm00442104_m1	human *WNT8a*	Hs00230534_m1
mouse *Wnt11*	Mm00437328_m1	human *WNT8b*	Hs00610126_m1
mouse *Wnt16*	Mm00446420_m1	human *WNT9a*	Hs00243321_m1
mouse *Wnt2*	Mm00470018_m1	human *WNT9b*	Hs00287409_m1
mouse *Wnt2b*	Mm00437330_m1		
mouse *Wnt3*	Mm00437336_m1		
mouse *Wnt3a*	Mm00437337_m1		
mouse *Wnt4*	Mm01194003_m1		
mouse *Wnt5a*	Mm00437347_m1		
mouse *Wnt5b*	Mm01183986_m1		
mouse *Wnt6*	Mm00437353_m1		
mouse *Wnt7a*	Mm00437354_m1		
mouse *Wnt7h*	Mm01301717_m1		
mouse *Wnt8a*	Mm01157914_g1		
mouse *Wnt8b*	Mm00442107_m1		
mouse *Wnt9a*	Mm00460518_m1		
mouse *Wnt9b*	Mm00457102_m1		